JMEPEG (1993) 2:333-340

Modeling of the Consolidation of Continuous-Fiber Metal Matrix Composites via Foil-Fiber-Foil Techniques

R.L. Goetz, W.R. Kerr, and S.L. Semiatin

The consolidation of metal-matrix composites (MMC) via hot isostatic pressing (HIP) of foil-fiber-foil layups has been investigated using finite element method (FEM) metal flow analysis. For this purpose, the deformation pattern for various fiber arrangements was determined using representative unit cells to describe extremes in behavior. For a given fiber architecture, the consolidation time was found to be heavily dependent on the ratio of the HIP pressure to average flow stress and the friction conditions at the matrix-fiber interface. The specific influence of material properties such as the rate sensitivity of the flow stress appears to enter only as a second order effect. The FEM solutions were used to construct HIP diagrams delineating temperature-time-pressure combinations for full composite consolidation. Laboratory trials on subscale foil-fiber coupons were used to validate the FEM predictions.

Keywords

consolidation, FEM process modeling, foil-fiber-foil, hot isostatic pressing, metal matrix composites

1. Introduction

METAL matrix composites (MMC) with continuous-fiber reinforcements are being considered as prime candidates for the next generation of high-temperature materials. If developed and implemented successfully, MMC's offer an attractive blend of high strength, high stiffness, and low density with tailored toughness and creep resistance. One of the most important steps in transitioning these materials to service is the development of cost-effective processing methods. To date, most of the effort in this area has focused on hot isostatic pressing (HIPing) or vacuum hot press consolidation of the discrete components (e.g., the foil-fiber-foil and powder cloth techniques) or layups of monotapes containing both matrix and fiber constituents made by techniques such as tapecasting, plasma spray, or other deposition approaches. It is not surprising that processing parameters such as temperature, time, and pressure are important in the design of optimal practices. For example, temperature and time both affect the degree and rate of reaction between the fibers and matrix. The pressurization cycle during consolidation can affect the tendency for fiber breakage and control of fiber spacing. Furthermore, because of the difference in thermal expansion coefficients between the fiber and the matrix, peak consolidation temperature strongly impacts the level of residual stresses that are developed during cooldown following the actual consolidation.

Although the consolidation of real MMC components involves a wide range of considerations, from tooling/can design, parting agents, and fixturing to equipment design and selection of detailed pressurization and heating cycles, broad insight into the scientific aspects of consolidation can be obtained from relatively straightforward modeling techniques and laboratory coupon tests. The thrust of the present work had such a basic focus. Specifically, the HIP consolidation behavior of MMC's made via the foil-fiber-foil method was studied by finite element modeling (FEM) of the metal flow around rigid fibers. Model calculations were performed for composites consisting of an alpha-two titanium aluminide matrix containing silicon carbide fibers. Details of the matrix deformation, including strain and strain rate fields, were investigated. In addition, consolidation times were predicted as a function of HIP temperature and pressure, fiber architecture, and interface friction between the matrix and fiber. These latter results were summarized in the form of HIP diagrams.

R.L. Goetz, UES, Inc., Dayton, Ohio; **W.R. Kerr** and **S.L. Semiatin,** Materials Directorate, Wright Laboratory, WL/MLLN, Wright-Patterson AFB, Ohio.

2. Background

To place the present work in a proper context, previous efforts in the area of modeling of MMC consolidation will be summarized. Prior investigations have included a variety of analytical and numerical approaches. Early analytical models were developed by Wilkening and Backofen,[1] Chang and Scala,[2] and Shorshorov et al.[3] In all cases, the matrix material was assumed to be rigid, rate insensitive, and perfectly plastic (i.e., have a constant flow stress), deformation was assumed to be plane strain, and matrix-fiber friction was taken into account using either a friction shear factor or Coulomb friction factor. Because the materials were assumed to be rigid-plastic, the main output in each case was the ratio of the pressure to bring about complete metal flow between the fibers to the material flow stress.

The Wilkening and Backofen approach, based on extrusion of the matrix between the fibers, gave results as a function of fiber spacing. Chang and Scala derived slab model results that were similar to those of Wilkening and Backofen. Using an upper bound approach, Chang and Scala also derived predictions for the pressure-flow stress ratio for simulated MMC consolidation processes based on either indentation of fibers in composite monolayers, or the deformation of matrix material extruded between two fibers. The validity of model predictions was established by pressing steel drill rods into aluminum alloy 1100-H14 sheets. It was found that the upper bound indentation model gave the best agreement with the measurements; the up-

per bound extrusion model greatly overestimated the required pressures, whereas the slab model and the Wilkening and Backofen model underestimated the required pressures.

In yet further studies, Chang and Scala developed an upper bound model for consolidation of multilayer composites. This model revealed the effects of fiber packing arrangement and platen/composite layup friction/hill phenomena. It was found that the predicted pressure does not depend explicitly on fiber volume fraction, but that the form of the velocity discontinuities within the matrix (between the fibers) strongly affects the required pressure as does the composite width-to-thickness ratio.

Shorshorov et al.[3] developed a model similar to the upper bound extrusion approach of Chang and Scala. The analysis took into account the work of matrix deformation and that due to fiber-matrix friction, as well as the work to deform asperities during the final stages of consolidation in which matrix material is actually bonded between the fibers. Model predictions were found to markedly overestimate measured pressures for consolidation of a boron fiber-aluminum alloy monolayer composite.

More recent models of composite consolidation have also dealt largely with monolayer foil-fiber-foil geometries. Nicolaou, Piehler, and Kuhni[4] used a simple axial force balance to illustrate at least qualitatively how the ratio of applied pressure to material flow stress varies during the hot press consolidation cycle for a rate-sensitive (power law creep) material. As the contact area between the fibers and matrix increases during consolidation, the average stress decreases (for a fixed applied pressure), resulting in decreasing strain rate and thus retarded densification near the end of the cycle. This qualitative insight was verified by experimental observations,[4] as well as subsequent numerical calculations using the FEM program ABAQUS.[5] This latter work was used to develop maps showing the predicted densification at fixed temperature as a function of applied pressure and time.

Bampton et al.[6] used a simple analytical equilibrium-based technique to estimate consolidation times for monolayer foil-fiber-foil composites whose matrices were assumed to deform by creep. The effect of fiber spacing and temperature was examined by this method for several intermetallic matrix composites.

Semiatin, Goetz, and Kerr[7] used advanced numerical techniques, i.e., the FEM program ALPID, to analyze the consolidation of foil-fiber-foil composites. In contrast to previous work, these simulations treated multilayer fiber arrangements. The material constitutive behavior was assumed to be rate sensitive; a power law creep formulation was used. The effect of consolidation temperature on foil deformation patterns was determined. In addition, some initial model results for the times for partial and complete consolidation as a function of temperature and pressure were presented for an alpha-two (Ti-24Al-11Nb, at.%), silicon carbide composite. The effort described below provides more recent results and interpretation of the kinetics of consolidation, a comparison of rate-sensitive model results to those from the Chang and Scala rate-insensitive for-

Table 1 Material coefficients for Ti-24Al-11Nb[9]

Temperature, °C	*K*, MPa	*m*
650	550	0.10
760	940	0.21
870	1090	0.31
980	4120	0.62

Note: $\dot{\bar{\varepsilon}} = 4 \times 10^{-5}$ to 2×10^{-3} s^{-1}.

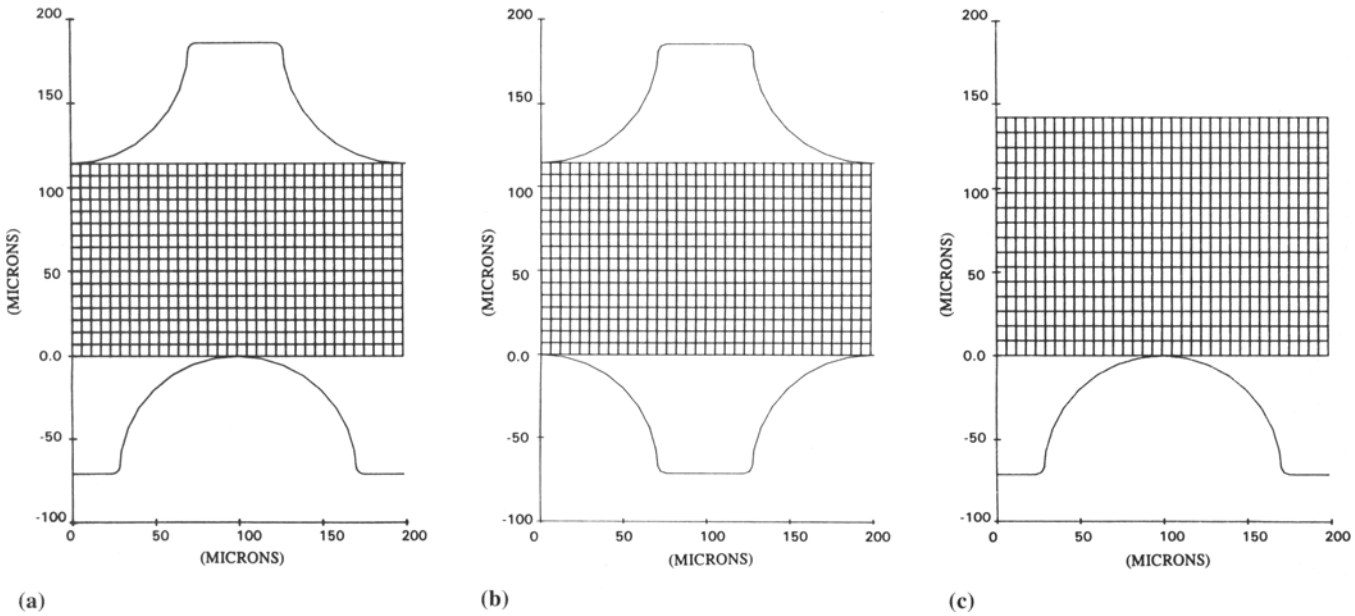

Fig. 1 Initial FEM grids for the three unit cells. (a) Triangular, (b) square, and (c) monolayer. Foil thickness, 115 μm (a and b) or 142 μm (c); fiber diameter, 142 μm; fiber center-to-center spacing, 198 μm.

mulation, and an experimental validation of the numerical FEM predictions for foil-fiber-foil consolidation.

3. Approach

The two-dimensional FEM code ALPID[8] was used in the present work to model the HIP consolidation of multilayer foil-fiber-foil composites under isothermal plane-strain conditions. Although ALPID is capable of simulating nonisothermal processes, idealized constant pressure, constant temperature conditions were assumed in the present work to separate out the complex transient effects associated with scaled up processes from the basic material behavior of interest here. Moreover, the strain rates involved were low enough to assume that deformation heating would give rise to negligible temperature increases in the deforming foil. The silicon carbide fibers were modeled as rigid dies in the simulations. As in the previous investigation,[7] the matrix material was taken to be the alpha-two titanium aluminide (Ti-24Al-11Nb, at.%), whose constitutive equation was fit to the simple power law formulation, $\bar{\sigma} = K\dot{\bar{\varepsilon}}^{m}$. To a good approximation, the material coefficients K and m were constant over the strain rate range of interest at a given temperature. The temperature dependence is summarized in Table 1.

It is not possible to model the actual consolidation problem by including every fiber, nor is it necessary because of reoccurring fiber patterns. Although in practice there is some variability in fiber arrangement, the majority are arranged as modeled by the three unit cells, triangular, square, and monolayer, shown in Fig. 1. A fourth unit cell in which two fibers have moved together has also been examined, but will not be discussed here. Recent work[10] has demonstrated that movement of fibers so that they touch or move apart, i.e., fiber swimming, most likely does not occur during the actual consolidation events, but rather during the initial pressurization stage (when the foils deform elastically). This swimming results from geometrical considerations related to fiber mat weaving practice. A limited number of computer simulations were also conducted for monolayer foil-fiber layups to obtain results that could be compared to the analytical model of Chang and Scala.[2]

For the unit cells shown in Fig. 1, the foil thickness was 115 μm, except for the monolayer unit cell which used a foil thickness of 142 μm. The fiber diameter was 142 μm, and the center-to-center fiber spacing was 198 μm. Additional fiber spacings of 284 and 350 μm were used in the monolayer unit cell simulations. The foil deformation was analyzed using a mesh consisting of 544 four-node quadrilateral elements connected at 595 nodes. The left and right vertical foil planes were assumed to undergo no displacement in the horizontal direction (due to symmetry considerations). At the foil-fiber interfaces, a constant friction shear factor ($M = 0.1$ or 1.0) boundary condition was imposed. The boundary conditions on the rigid fibers, which were treated like dies, consisted of the specification of a constant average surface traction along the top and bottom. For the version of ALPID that was used here, only velocity boundary conditions could be specified. Thus, the velocity was checked and modified as necessary after each increment of deformation to ensure the constancy of load. The correction was based on the constitutive equation of the foil alloy, or more specifically the strain-rate sensitivity m, according to the relation:

$$V_u / V_c = \left(F^* / F_c\right)^{1/m} \qquad [1]$$

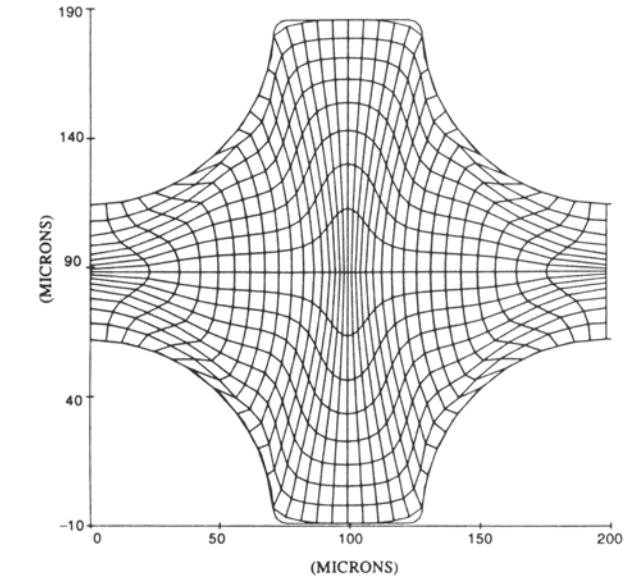

(a)

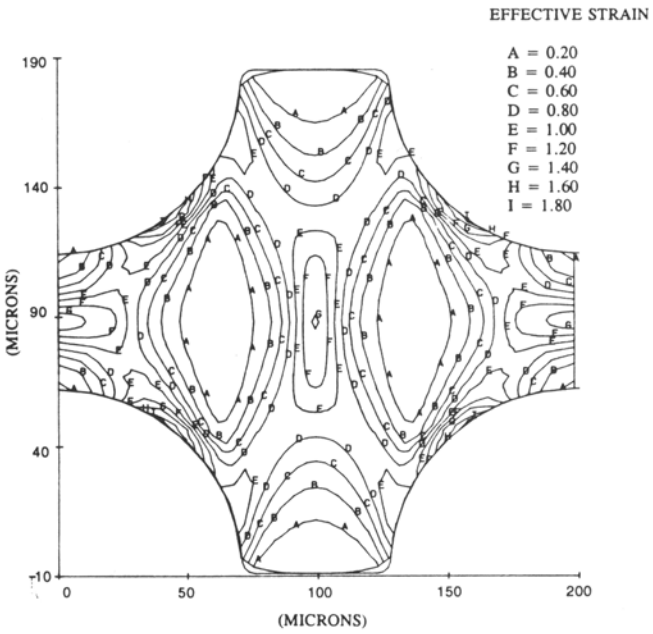

(b)

Fig. 2 FEM-predicted metal flow for a square unit cell after HIP consolidation for 4.2 h at 650 °C under a pressure of 415 MPa, assuming a friction factor of $M = 1.0$. (a) Grid distortions. (b) Strain contours.

where V_c, V_u are the current and "updated" displacement rate; F^* is the desired (constant) force; and F_c is the (calculated) force applied during the current deformation step.

Consolidation was considered to be complete when the foil contacted the top and bottom symmetry planes (i.e., the bond line) and the final pore closure at the ends of the bond line, next to the fiber, had been completed. The actual microscopic bonding processes (e.g., deformation of asperities) that characterize diffusion bonding of flat sheets[11] were neglected for the present; analysis of such phenomena is currently underway.

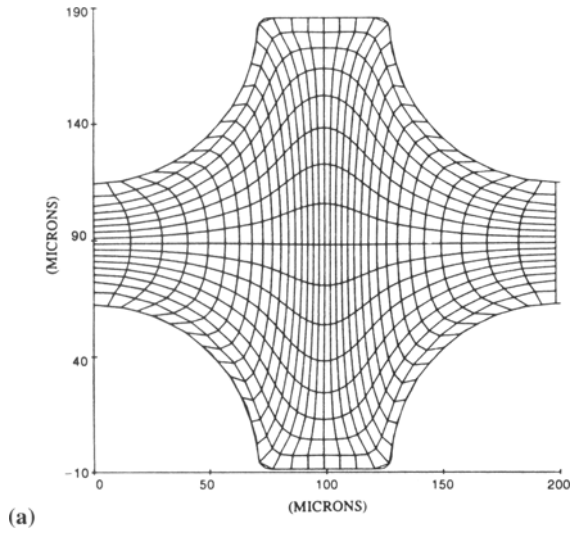

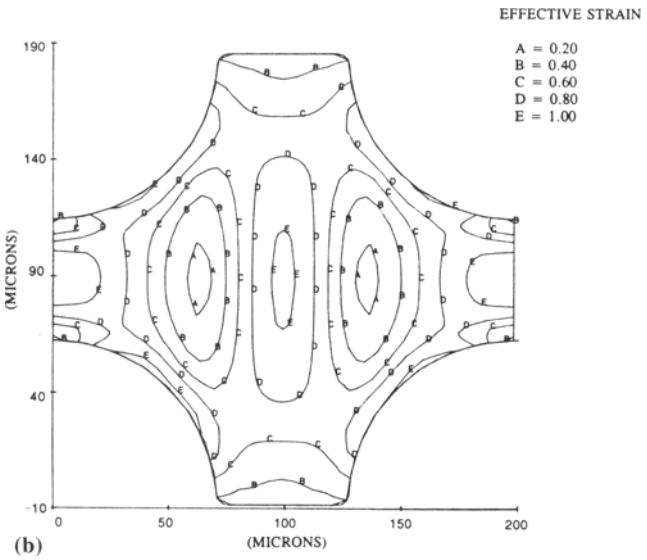

Fig. 3 FEM-predicted metal flow for a square unit cell after HIP consolidation for 0.45 h at 980 °C under a pressure of 70 MPa, assuming a friction factor of $M = 1.0$. (a) Grid distortions. (b) Strain contours.

4. Discussion and Results

The FEM results are discussed below in terms of metal flow predictions, consolidation time and pressure requirements, and HIP diagrams for foil-fiber-foil consolidation.

4.1 *Metal Flow Predictions*

Predicted metal flow patterns were found to be a strong function of consolidation temperature. For instance, the matrix flow behavior for a square unit cell under two extreme conditions is summarized in Fig. 2 and 3. At the lower temperature of 650 °C (Fig. 2), greater flow localization is observed than at 980 °C (Fig. 3). At 650 °C, the peak strain is 1.8, whereas it is only 1.0 at 980 °C. This is caused by the low strain-rate sensitivity (0.1) at 650 °C. By comparison, the rate sensitivity at 980 °C is 0.62. The same effect was observed with the triangular unit cell, as shown by Semiatin et al.[7] It is also of interest to note that the predicted strain in the region where adjacent foils bond is approximately 0.4, or a level of deformation that might be expected to be sufficient to break up residual surface oxide layers and enhance bonding.

The area-weighted average effective strain, $\bar{\varepsilon}_{av}$, was calculated from the simulations by summing the products of the individual element areas and element effective strains and dividing this sum by the total area. For a given type of unit cell, it was found that the final average strain was independent of consolidation temperature and hence strain-rate sensitivity, despite the marked differences in flow uniformity noted above. Although processing conditions do not appear to affect the average strain for a given unit cell, differences were found between the square and triangular cell. At full consolidation, the average strain for the square cells was 0.65, and that for the triangular cells was 0.55. This difference is further illustrated in Fig. 4, in which the

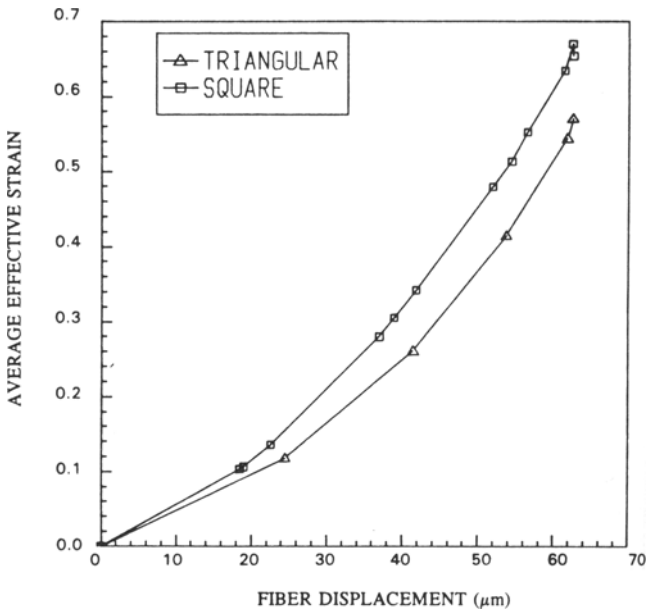

Fig. 4 FEM-predicted average matrix strain for triangular and square unit cells as a function of fiber displacement, assuming $M = 1.0$. A displacement of 62 μm yields full consolidation.

instantaneous average strain as a function of fiber displacement is plotted.

4.2 *Engineering Estimates of Required Consolidation Time/Pressure*

An approximate method to estimate the required consolidation time or pressure at a given temperature was developed based on the results of the FEM simulations. The method hinges on the definition of an average effective strain rate for the initial 97% of the consolidation process. As discussed by Semiatin et al.,[7] at a given temperature and pressure, the time to complete the first 97% of the consolidation, denoted t^*, is approximately equal to that for the remaining 3%. The average effective strain rate, $\dot{\bar{\varepsilon}}^*$, is defined as the average effective strain (e.g., 0.65 for the square unit cell and 0.55 for the triangular unit cell of the present geometry) divided by t^*. An average flow stress, $\bar{\sigma}^*$, is then defined from the constitutive relation $\bar{\sigma}^* = K\dot{\bar{\varepsilon}}^{*m}$.

With the average flow stress thus defined, the ratio F of the HIP pressure P_H to $\bar{\sigma}^*$ was estimated from the FEM simulations for consolidation of the Ti-24Al-11Nb/silicon carbide composites under a wide range of pressure and temperature combinations. The results (Fig. 5) show a surprising insensitivity to HIP temperature (and thus rate sensitivity), but a strong dependence on friction shear factor M. For $M = 0.1$, $F = P_H/\bar{\sigma}^*$ was found to be equal to approximately 1.27, whereas for $M = 1.0$, it was about 1.61.

Using the ratio $F = F(M)$, an engineering estimate of the required pressure P_H for given consolidation time, denoted t_c, and temperature, T, or the required time at a given pressure and temperature can readily be obtained from the following relations, after noting that $t_c \approx 2t^*$:

$$P_H = F(M)\bar{\sigma}^* = F(M)K(T)\dot{\bar{\varepsilon}}^{*m} \quad [2]$$

or

$$P_H = F(M)K(T)(\bar{\varepsilon}_{av}/t^*)^m \approx F(M)K(T)(2\bar{\varepsilon}_{av}/t_c)^m \quad [3]$$

for the required pressure. Inverting Eq 3 yields an expression for the consolidation time, t_c, as a function of HIP pressure, P_H:

$$t_c \approx 2\bar{\varepsilon}_{av}[F(M)K(T)/P_H]^{1/m} \quad [4]$$

Thus, once the foil material properties (i.e., K and m) are known as a function of temperature, the relation between consolidation pressure and time is readily derived from Eq 3 or Eq 4 using appropriate values for $F(M)$ and $\bar{\varepsilon}_{av}$.

4.3 *Comparison of Rate-Insensitive and Rate-Sensitive Consolidation Behavior*

The finite-element method was also applied to obtain results for rate-sensitive matrix materials that could be compared directly to the results obtained by Chang and Scala[2] for rate-insensitive materials using the upper bound method of plasticity. The FEM solutions were carried out to simulate the flow of the Ti-24Al-11Nb matrix between the silicon carbide fibers (Fig. 1c). The center-to-center spacing of 142-μm diameter fibers was assumed to be 198 μm (interfiber distant = 56 μm), 284 μm

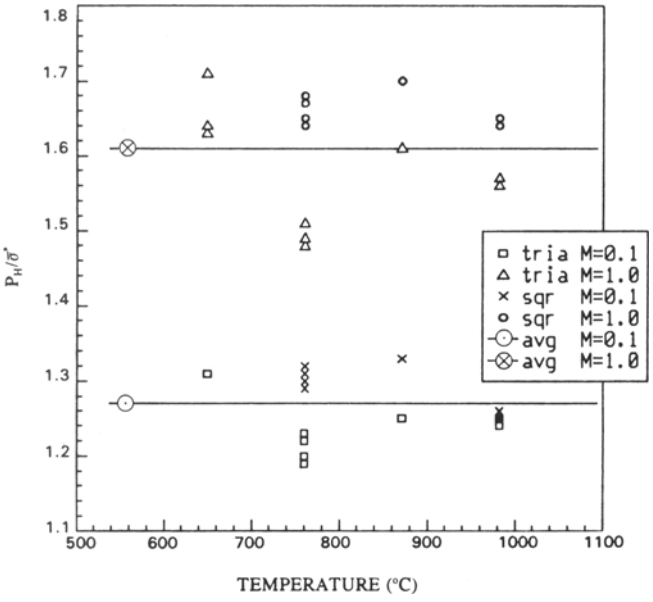

Fig. 5 FEM-predicted ratio of HIP pressure, P_H, to average foil flow stress $\bar{\sigma}^*$ after 97% consolidation for various temperatures, friction conditions of $M = 1.0$ (average $P_H/\bar{\sigma}^* = 1.61$) or $M = 0.1$ (average $P_H/\bar{\sigma}^* = 1.27$), and the square and triangular unit cells.

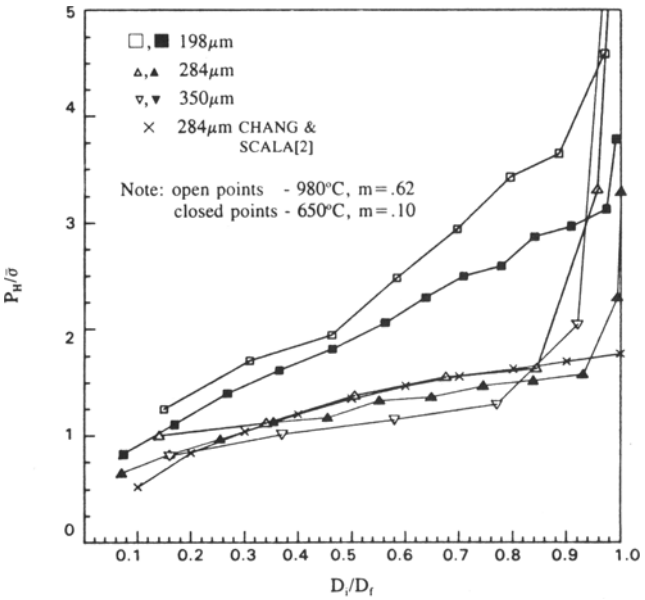

Fig. 6 FEM-predicted variation in the ratio $P_H/\bar{\sigma}$ as a function of fiber displacement for a friction factor of 1.0 and a monolayer layup of various geometries. D_i is the instantaneous fiber displacement, and D_f is the displacement for full consolidation.

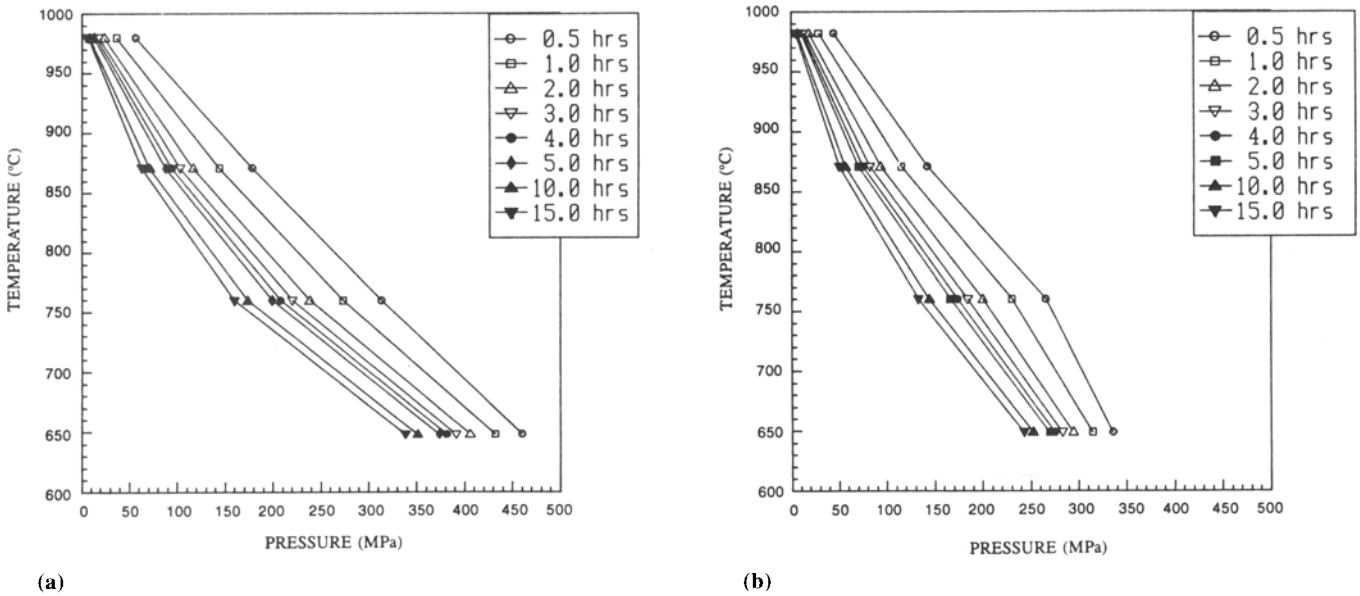

Fig. 7 FEM-generated HIP diagram for full consolidation of Ti-24Al-11Nb/SiC foil-fiber-foil composites assuming a triangular unit cell. (a) $M = 1.0$. (b) $M = 0.1$.

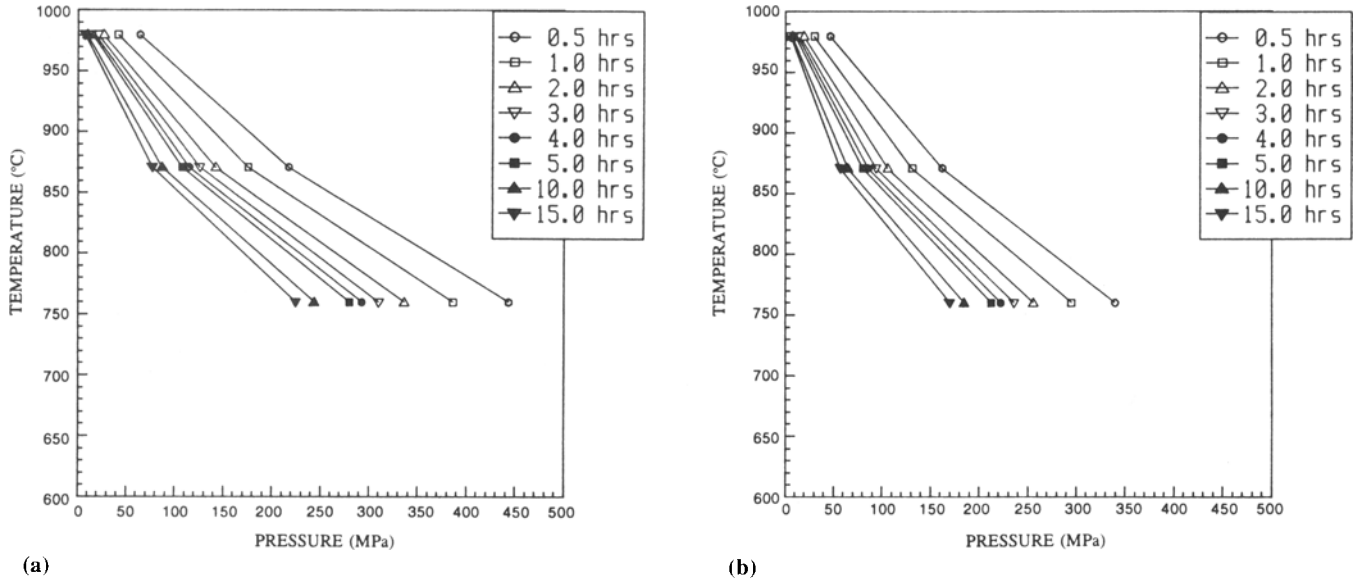

Fig. 8 FEM-generated HIP diagram for full consolidation of Ti-24Al-11Nb/SiC foil-fiber-foil composites assuming a square unit cell. (a) $M = 1.0$. (b) $M = 0.1$.

(interfiber distance = 142 μm), or 350 μm (interfiber spacing = 208 μm). The foil thickness was taken to be the same as the fiber diameter, or 142 μm. Calculations were done for two sets of consolidation conditions (two temperatures, 650 and 980 °C; one friction shear factor, $M = 1.0$) for each fiber spacing.

The output of the FEM simulation was summarized in terms of the instantaneous value of $P_H/\bar{\sigma}$ as a function of fiber displacement, where $\bar{\sigma}$ was the instantaneous area-weighted effective flow stress. The results are shown in Fig. 6. Focusing on the FEM results initially, it is observed that the predicted values of $P_H/\bar{\sigma}$ for a given fiber spacing are insensitive to the HIP temperature (and hence m value), in agreement with the findings above. By contrast, the overall magnitudes of $P_H/\bar{\sigma}$ increase markedly as the fiber spacing is decreased. This trend reflects the effects of increased reduction and redundant work on the deformation resistance.

The Chang and Scala results for the indentation model with an interfiber distance equal to the fiber diameter are also plotted in Fig. 6. It should be noted that the Chang and Scala results are for $P_H/\bar{\sigma}$ versus the ratio of fiber depth embedded in matrix to

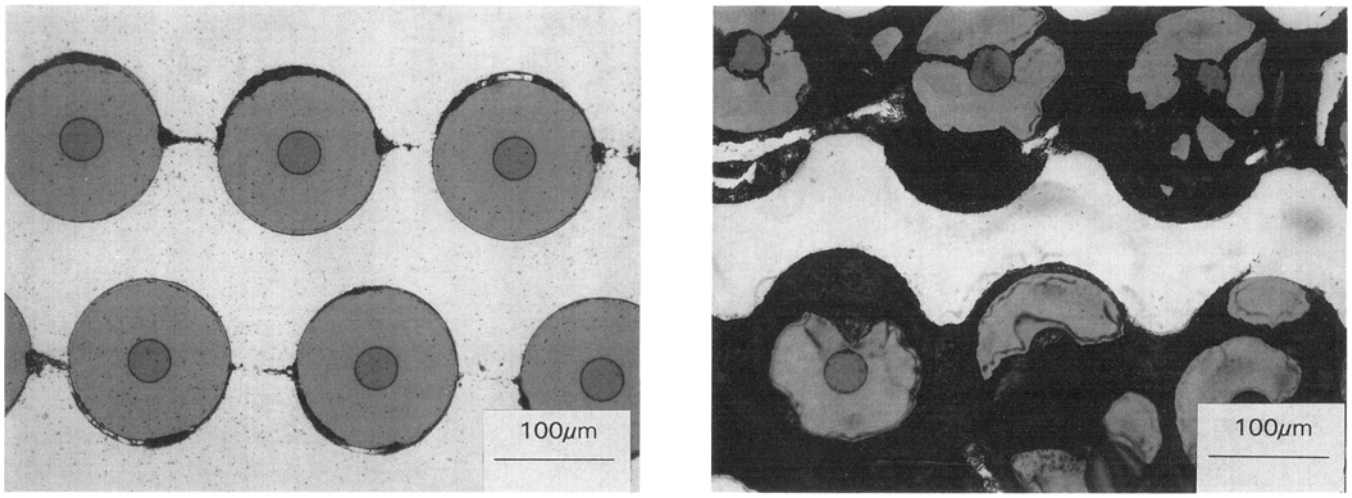

(a) (b)

Fig. 9 Optical micrographs of Ti-24Al-11Nb/SCS-6 foil-fiber-foil layups after HIP consolidation at 980 °C, 70 MPa for (a) 40 min or (b) 20 min.

Table 2 Consolidation equation parameters for Ti-24Al-11Nb/SiC composites

Temperature, °C	Friction factor, *M*	Square unit cell		Triangular unit cell	
		B	*a*	*B*	*a*
650	0.1	...	...	$1.96(10)^{26}$	−10.53
	1.0	...	...	$1.48(10)^{29}$	−11.07
760	0.1	$1.31(10)^{12}$	−4.90	$3.82(10)^{11}$	−4.90
	1.0	$8.58(10)^{12}$	−5.00	$2.25(10)^{12}$	−5.07
870	0.1	$8.69(10)^{6}$	−3.27	$5.59(10)^{6}$	−3.27
	1.0	$2.26(10)^{7}$	−3.27	$1.14(10)^{7}$	−3.27
980	0.1	$2.43(10)^{2}$	−1.61	$2.24(10)^{2}$	−1.61
	1.0	$4.06(10)^{2}$	−1.61	$3.30(10)^{2}$	−1.61

Note: $t_c(\text{hours}) = B\,P_H(\text{MPa})^a$.

fiber radius instead of fiber displacement to final fiber displacement. In the present work, the matrix simultaneously fills the fiber gap as the fiber moves so the fiber displacement will always be less than the fiber diameter, which is different from the Chang/Scala indentation model. Regardless of this difference, agreement with the FEM model is reasonably good. Therefore, it may be surmised that rate sensitivity effects *per se* play a lesser role in determining consolidation pressure compared to geometric effects and matrix-fiber interface friction, a conclusion drawn from the results of the previous section as well.

4.4 *HIP Diagrams*

Diagrams relating combinations of temperature, time, and pressure for foil-fiber-foil consolidation via HIP were also derived from the FEM simulations. These HIP diagrams are similar in nature to those used to describe consolidation of powder metals and ceramics.[12] Figures 7 and 8 are the FEM-calculated HIP diagrams for triangular and square unit cell geometries, respectively, for Ti-24Al-11Nb/silicon carbide composites. The composites in these cases consist of 114-μm thick foil and fiber mats comprised of 142-μm diameter fibers with a 198-μm center-to-center spacing. An analytical expression has been fit to the results to predict the relationship between consolidation time (t_c), HIP pressure (P_H, in MPa), and temperature:

$$t_c(\text{hours}) = B\,P_H{}^a$$

where B and a are functions of temperature, friction factor, and unit cell geometry (Table 2). The values of the pressure exponent (a) are very similar to those of $-1/n$ at a given temperature (Table 1), a trend indicating the reasonableness of the curve fit in reproducing the overall rate effects important in the consolidation process.

4.5 *Validation of HIP Diagram Calculations*

A number of HIP consolidation trials were performed to validate the FEM approach for the modeling of foil-fiber-foil MMC fabrication. To approximate the isothermal, isobaric conditions of the numerical model, experimental HIP runs were conducted using small coupons (approximately 10 × 25 mm in plane area). The temperature and pressure in the HIP vessel

were ramped up together to a temperature approximately 100 °C below the desired peak temperature, at which point the pressure was increased to the desired peak pressure. Once this pressure was reached, the temperature of the HIP vessel was raised as quickly as possible to the peak temperature, and consolidation was allowed to occur for varying amounts of time.

Representative observations from HIP experiments conducted at a temperature of 980 °C and a pressure of 70 MPa are shown in Fig. 9. The layup that was HIP processed for 40 min (Fig. 9a) shows essentially full consolidation. On the other hand, a layup exposed for only 20 min at the same pressure and temperature (Fig. 9b) exhibits large amounts of metal flow, but an absence of bonding. The rounded edges of the foil at the incipient bond line suggest consolidation approaching 90 to 95%, with adjacent foils just coming into contact at the point the HIP run was stopped.

These experimental observations can be compared to the predictions of the HIP diagram for the square unit cell (Fig. 8a), the geometry that gives rise to the more conservative estimate of required HIP time. Assuming $M = 1.0$ (matrix sticking to fiber when contact is made), the HIP diagram predicts a consolidation time of approximately 30 min, in broad agreement with experimental observations.

5. Summary and Conclusions

The detailed features of metal flow during MMC consolidation via foil-fiber-foil techniques were established using the finite element method. Although the strain-rate sensitivity of the flow stress affects the uniformity of metal flow during consolidation, the average effective strain experienced by the foil is principally determined by the fiber arrangement and not by specific material properties. For this reason, the ratio of HIP pressure to average flow stress in the matrix is dependent predominantly on the frictional conditions at the matrix-fiber interface for a given fiber arrangement. This enables the determination of approximate HIP pressures from specified HIP times and temperatures (which determine an average matrix flow stress) or conversely HIP time from specified HIP pressure and temperature, provided a material flow stress data base is available for the foil alloy. More detailed summaries of the FEM results were collected in the form of HIP diagrams. Experimental HIP runs were used to establish the validity of the HIP diagrams for Ti-24Al-11Nb/SiC foil-fiber-foil composite consolidation.

Acknowledgments

This work was conducted as part of the in-house research activities of the Air Force Materials Directorate Processing Science Group. One of the authors (RLG) was supported under the auspices of Contract No. F33615-C-92-5900 during the course of this work. The materials used in this research were graciously supplied by Texas Instruments, Inc. and Textron Specialty Materials. Discussions with Dr. Israil Sukonnik of Texas Instruments and Dr. Clifford Bampton of Rockwell International Science Center during the course of this work are appreciated.

References

1. W.W. Wilkening and W.A. Backofen, "Deformation Processing of Anisotropic Metals," Final Report, Contract N00019-70-C-0071, Massachusetts Institute of Technology, Cambridge, Aug 1970
2. M. Chang and E. Scala, Plastic Deformation Processing and Compressive Failure Mechanism in Aluminum Composite Materials, *Composite Materials: Testing and Design (Third Conference), ASTM STP 546*, American Society for Testing and Materials, 1974, p 561-579
3. M.Kh. Shorshorov, V.A. Kolesnichenko, and R.S. Yusupov, Calculation of Hot-Pressing Pressure for Composite Fiber Materials, *Sov. Powder Metall. Met. Ceram.*, Vol 20(No. 7), 1981, p 461-465
4. P.D. Nicolaou, H.R. Piehler, and M.A. Kuhni, Fabrication of Ti-6Al-4V Matrix, SCS-6 Fiber Composites by Hot Pressing Using the Foil/Fiber/Foil Technique, *Developments in Ceramics and Metal Matrix Composites*, K. Upadhya, Ed., The Minerals, Metals, and Materials Society, 1992, p 37-47
5. P.D. Nicolaou, "Fabrication of Continuous Fiber Metal Matrix Composites Using the Foil/Fiber/Foil Technique," unpublished research, Carnegie Mellon University, July 1992
6. C.C. Bampton, J.A. Graves, K.J. Newell, and R.H. Lorenz, Process Modeling for Titanium Aluminide Matrix Composites, *Intermetallic Matrix Composites II*, D.B. Miracle, D.L. Anton, and J.A. Graves, Ed., Materials Research Society, Vol 273, 1992, p 365-376
7. S.L. Semiatin, R.L. Goetz, and W.R. Kerr, Consolidation of Continuous Fiber Intermetallic Matrix Composites, *Intermetallic Matrix Composites II*, D.B. Miracle, D.L. Anton, and J.A. Graves, Ed., Materials Research Society, Vol. 273, 1992, p 351-364
8. S.I. Oh, Finite Element Analysis of Metal Forming Problems with Arbitrarily Shaped Dies, *Int. J. Mech. Sci.*, Vol 24, 1982, p 479
9. C.C. Bampton, unpublished research, Rockwell International Science Center, Thousand Oaks, CA, 1991
10. W.R. Kerr, unpublished research, Air Force Materials Directorate, Wright Laboratory, Wright-Patterson Air Force Base, 1992
11. G. Garmong, N.E. Paton, and A.S. Argon, Attainment of Full Interfacial Contact During Diffusion Bonding, *Metall. Trans. A*, Vol 6, 1975, p 1269-1279
12. A.S. Helle, K.E. Easterling, and M.F. Ashby, Hot-Isostatic Pressing Diagrams: New Developments, *Acta Metall.*, Vol 33, 1985, p 2163-2174